Bulletin of Electrical Engineering and Informatics
Vol. 15, No. 6, December 2026, pp. 4802~4814
ISSN: 2302-9285, DOI: 10.11591/eei.v15i6.13860

ANFIS based photovoltaic interconnected smart grid with power quality improvement

Jabinbanu Mahaboobsab Nadaf[1], Sudarshana Reddy Handihal Rukmangada[2,3], Suresh Haleyur Lakshmegowda[4]
[1]Department of Electrical Engineering, Sri Channakeshava Government Polytechnic, Bankapur and Visvesvaraya Technological University, Belgaum, India
[2]Regional Office Bengaluru, Visvesvaraya Technological University, Bengaluru, India
[3]Department of Electrical and Electronic Engineering, University BDT College of Engineering, affiliated to Visvesvaraya Technological University, Davangere, India
[4]Department of Electrical and Electronics Engineering, Sir M Visvesvaraya Institute of Technology, Bengaluru, India

Article Info

Article history:

Received Jul 2, 2026
Revised Sep 21, 2026
Accepted Oct 4, 2026

Keywords:

ANFIS
Grid instability
Micro-grid
Photovoltaic power
UPQC
Validation of UPQC

ABSTRACT

Maintaining power quality is a critical challenge when using microgrids as a primary power source, largely due to their reliance on intermittent renewable energy. During peak loading conditions, these power fluctuations can lead to significant grid instability. The instability is mainly voltage deviations, which are sag, unbalancing and swell. To address this, this article proposes an adaptive neuro-fuzzy inference system (ANFIS) controlled unified power quality conditioner (UPQC), supported directly by photovoltaic (PV) generation. The performance of this intelligent UPQC system is evaluated under standard environmental conditions, with MATLAB 2017b used to simulate and plot the system's effectiveness in mitigating power quality issues.

This is an open access article under the CC BY-SA license.

Corresponding Author:

Jabinbanu Mahaboobsab Nadaf
Department of Electrical Engineering, Sri Channakeshava Government Polytechnic
Bankapur and Visvesvaraya Technological University
Belgaum, India
Email: jabinbanu.nadaf5976@gmail.com

1. INTRODUCTION

The increasing penetration of nonlinear loads, renewable energy resources, and power-electronic interfaced devices has considerably degraded power quality in modern distribution systems. Conventional mitigation devices such as passive filters, dynamic voltage restorers (DVRs), and distribution static synchronous compensator (DSTATCOMs) are generally limited to either voltage or current compensation, making them insufficient for comprehensive power quality control. To overcome these limitations, the unified power quality conditioner (UPQC), which combines series and shunt active power filters, has emerged as an effective solution capable of simultaneously mitigating voltage sags/swells, current harmonics, reactive power imbalance, and load unbalance. Recent studies report significant advancements in UPQC topology, control strategies, switch-reduced configurations, and smart-grid-oriented applications, enhancing system reliability and dynamic performance [1]–[3]. The rapid growth of electric vehicle (EV) penetration has further intensified power quality challenges, particularly at EV charging stations due to their nonlinear, high-power, and stochastic charging characteristics. Research findings show that UPQC installed at the point of common coupling can effectively suppress harmonic currents, regulate voltage fluctuations, and improve power factor during both normal and fast-charging operations. Advanced control schemes, including hybrid

optimization techniques, moving window–based algorithms, and intelligent fuzzy-PI controllers, have demonstrated substantial reductions in total harmonic distortion (THD) and improved grid stability [4]–[8]. Moreover, the incorporation of vehicle-to-grid (V2G) functionality with UPQC enables bidirectional power flow, allowing EVs to support grid services while maintaining power quality compliance under dynamic operating conditions [9], [10]. Recent research has also focused on integrating UPQC with renewable and hybrid energy sources such as photovoltaic (PV) systems, wind energy, battery energy storage systems (BESS), and fuel cells to enhance power quality in microgrids and smart distribution networks. Fuel-cell-assisted UPQC architectures provide real-power support during grid disturbances and improve DC-link voltage regulation, ensuring continuous and effective compensation during supply interruptions [11], [12]. Additionally, data-driven and experimentally validated studies confirm that UPQC-based solutions significantly enhance voltage regulation, harmonic suppression, and system resilience in renewable-rich and EV-dominated grids, highlighting their critical role in future smart grid infrastructures [13].

Modern surveys emphasize that microgrids have evolved from simple islanded systems into intelligent, multi-layered energy networks with hierarchical and distributed control frameworks capable of operating in both grid-connected and islanded modes [14]. Advanced decentralized and hierarchical control architectures have been proposed to improve scalability, resilience, and plug-and-play capability, enabling seamless coordination among distributed energy resources (DERs), storage systems, and controllable loads [15]. Comprehensive monographs and textbooks further consolidate these developments by systematically addressing microgrid planning, design methodologies, protection schemes, and control layers [16].

In parallel, recent studies have highlighted the growing importance of integrating renewable energy sources into microgrids while maintaining operational stability and power quality. Reviews show that effective microgrid operation requires coordinated energy management strategies, advanced battery energy storage control, and dynamic power-sharing mechanisms to handle intermittency and load variability [17], [18]. Smart energy system concepts extend these ideas by embedding microgrids into broader smart city and smart grid frameworks, enabling bidirectional energy flow, real-time monitoring, and data-driven decision making [19]. Distributed and multi-agent control approaches have gained significant attention as they enhance system autonomy and reduce reliance on centralized controllers, particularly in large-scale and geographically dispersed microgrids [20].

Furthermore, recent literature extensively analyzes active and reactive power-sharing techniques to ensure voltage and frequency stability under varying generation and load conditions [21]. Centralized and hybrid optimization-based controllers have also been proposed to improve economic operation, reliability, and resilience of networked microgrids [22]. Finally, experimental validation using laboratory-scale and real-world microgrid testbeds has become a critical research direction, providing practical insights into controller implementation, communication challenges, and system dynamics under realistic operating conditions [23]. Collectively, these studies demonstrate that modern microgrids are transitioning toward intelligent, resilient, and flexible energy systems suitable for future smart grid applications. Although significant progress has been achieved in UPQC technology, conventional PI-based controllers often exhibit limited dynamic performance under rapidly changing operating conditions. Existing smart control approaches such as fuzzy logic and neural networks improve adaptability but may suffer from tuning complexity and uncertainty handling limitations. Furthermore, studies focusing on PV-integrated microgrids primarily address either renewable integration or power quality enhancement independently. Comprehensive intelligent frameworks capable of simultaneously managing voltage imbalance, reactive power compensation, harmonic suppression, and voltage regulation in PV-connected microgrids remain limited. Therefore, this work proposes an adaptive neuro-fuzzy inference system (ANFIS)-based UPQC framework that leverages both neural learning and fuzzy reasoning to achieve adaptive power quality enhancement under varying microgrid operating conditions.

In this paper, the validation of the UPQC which is controlled with ANFIS and power by PV solar is carried out in a standard test environment presented in [24], [25]. The UPQC is used here as power quality device and at the DC link the PV is used. The results are presented and compared with and without UPQC.

2. METHOD

The Figure 1 shows the proposed system. The Figure 1(a) shows the block diagram representation. At its core, the UPQC lies on two main components: the APF and the DVR regulators. The APF regulator actively monitors load voltages, capacitor voltage, and both load and injected currents. By processing these measurements, the APF algorithm generates the necessary compensation signals. These are then fed into a hysteresis controller to produce the required gate signals. On the other side, the DVR controller monitors supply voltages to detect sags or swells and generate its own voltage compensation signals, which are processed through a PWM controller to create the corresponding gate signals. Additionally, the system integrates a PV array as a DC grid. By adjusting the control strategy, this PV setup can seamlessly transition to act as an independent power source during islanded mode. Figure 1(b) shows the power flow of two different modes.

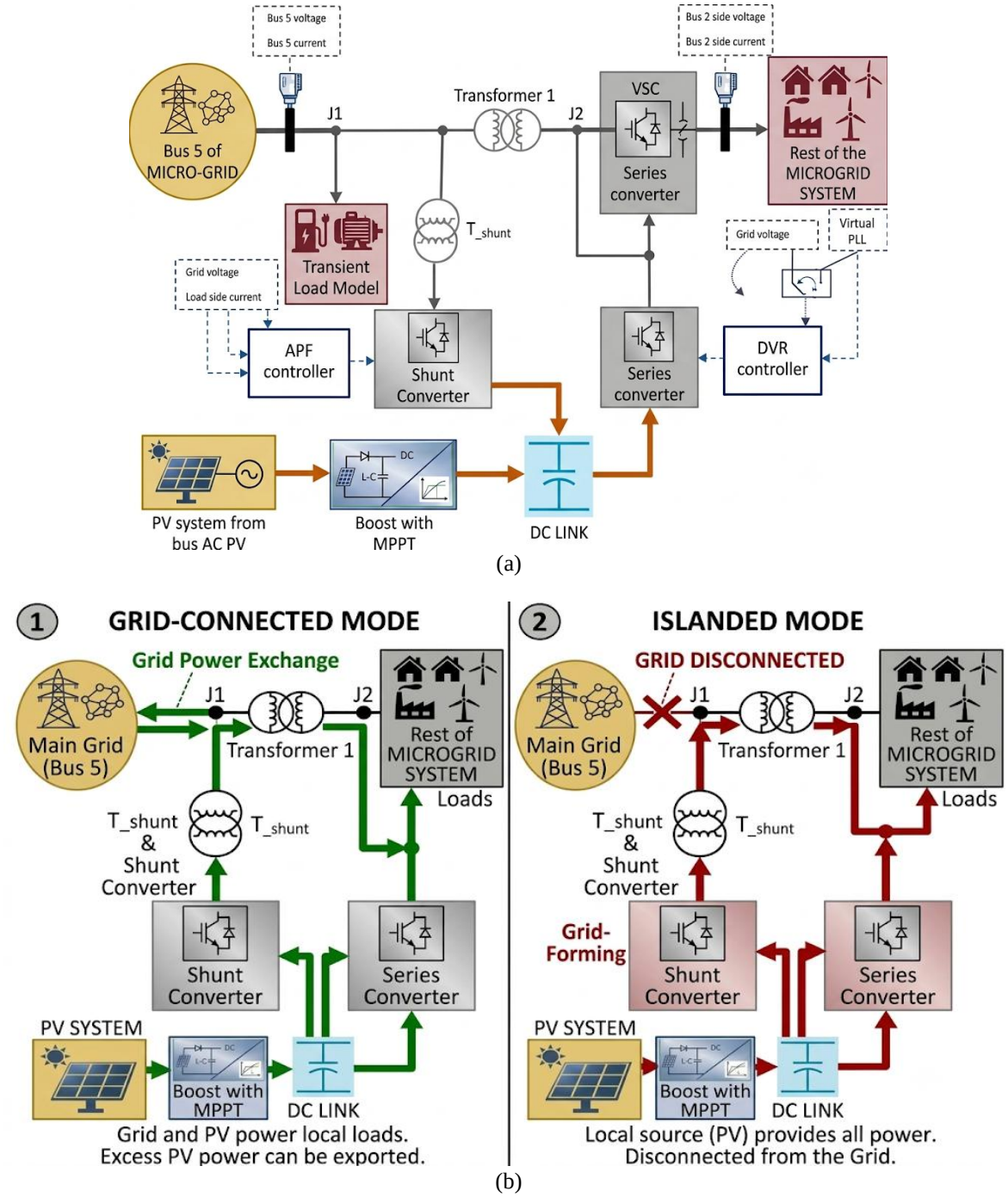


Figure 1. Proposed test system: (a) block diagram of proposed test system and (b) power flow diagram of grid-connected mode (arrow green) and islanded mode (arrow red)

2.1. Power quality assessment indices

The power quality indicators are; voltage unbalancing factors (VUF) (shows in (1)), power factor (shows in (2)), THD (shows in (3)), voltage sag (shows in (4)), voltage swell (shows in (5)), and reactive power (shows in (6)).

$$VUF(\%) = \frac{|V_2|}{|V_1|} \times 100 \quad (1)$$

Where, V_1 is positive sequence voltage and V_2 is negative sequence voltage.

$$PF = \frac{P}{S} \quad (2)$$

Where, P is active power (kW) and S is apparent power (kVA).

$$THD(\%) = \frac{\sqrt{\sum_{n=2}^{N} V_n^2}}{V_1} \times 100 \quad (3)$$

Where, V_1 is fundamental voltage component and V_n is nth harmonic component

$$Sag(\%) = \frac{V_{nom} - V_{sag}}{V_{nom}} \times 100 \quad (4)$$

$$Swell(\%) = \frac{V_{swell} - V_{nom}}{V_{nom}} \times 100 \quad (5)$$

$$Q = VI\sin\ \phi \quad (6)$$

Where, V is RMS voltage, I is RMS current, and ϕ is phase angle.

2.2. Measurement procedure

Power quality parameters were measured at all buses using MATLAB/Simulink measurement blocks. Voltage magnitude, current, active power, reactive power, and harmonic spectra were recorded before and after UPQC compensation. THD was calculated using fast Fourier transform (FFT) analysis over one fundamental cycle. Voltage imbalance was evaluated from phase voltages using symmetrical component analysis.

3. ANFIS CONTROL IN UNIFIED POWER QUALITY CONDITIONER

In the modeling and feedback control of dynamical systems, an effective controller is essential. It is responsible for mitigating external disturbances and rapidly restoring the plant to its steady-state or reference condition. Figure 2 shows the control diagram of the used ANFIS control. Table 1 shows the ANFIS control parameter and description.

$$e(k) = V_{dc}^{*} - V_{dc} \quad (7)$$

$$\Delta e(k) = e(k) - e(k-1) \quad (8)$$

Where V_{dc} ref is the reference voltage, Vdc is the actual voltage, e(k) is the error, and Δe(k) is the change in error.

The control process begins with the fuzzification unit, which translates crisp input data into linguistic variables. These variables are subsequently fed into a rule-based block containing 25 distinct rules derived from expert knowledge and empirical experience. To optimize the system's response, this rule base is integrated with a neural network trained via a backpropagation algorithm. This training phase is critical for dynamically selecting and tuning the most appropriate rule subset to formulate an accurate control signal.

Once the optimal rules are activated, the required control signal is generated. Ultimately, the ANFIS controller is driven by these fuzzified inputs, employing an inference mechanism that mirrors the robust decision-making processes found in traditional Mamdani and Takagi-Sugeno (TS) fuzzy logic controllers. For brevity, the specific 25 rules utilized in this framework are omitted from this paper.

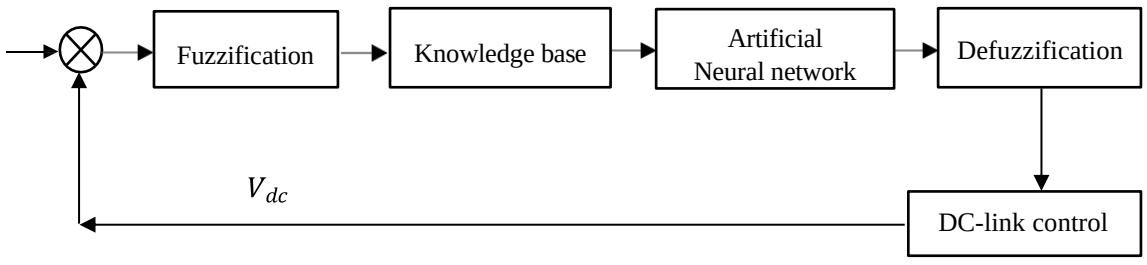


Figure 2. ANFIS implementation

Table 1. ANFIS control parameters and description

Parameters	Description
Input variables	$Input_1 = e(k)$ $Input_2 = \Delta e(k)$
Output variable	$u(k)$
ANFIS architecture	- Two inputs - Five Gaussian membership functions (MF) per input - 25 fuzzy rules - First-order TS structure - Hybrid learning algorithm
Training data	The training dataset was generated from the microgrid model under varying load demand, voltage sag, voltage swell, and harmonic distortion conditions. Approximately 1000 training samples were collected from offline simulations.
Training method	ANFIS parameters were optimized using a hybrid learning approach combining least-squares estimation for consequent parameters and backpropagation for premise parameters.
Reason for ANFIS	ANFIS was selected because it combines neural-network learning capability with fuzzy reasoning, providing improved adaptability under nonlinear and uncertain operating conditions compared with conventional PI, fuzzy logic, and fixed-gain controllers.

There are 5-MFs used here. For both inputs, e and Δe, the linguistic variables are as follows:

- NB–negative big
- NS–negative small
- ZE–zero
- PS–positive small
- PB–positive big.

Use Gaussian or triangular (Gaussian preferred for ANFIS) as shown in (9),

$$\mu(x) = exp\left(-\frac{(x-c)^2}{2\sigma^2}\right) \quad (9)$$

The MF distribution is given in Table 2. Table 3 shows the rule table used in the ANFIS controller. Here, H is high gain, M is medium gain, and L is low gain. Figure 3 shows the ANFIS structure which is built in MATLAB. Figure 4 shows the final rules used in the simulation as a 3D diagram.

Table 2. MF distribution

Label	Center (c)	Width (σ)
NB	-1	0.3
NS	-0.5	0.3
ZE	0	0.3
PS	0.5	0.3
PB	1	0.3

Table 3. Rule table

e\Δe	NB	NS	ZE	PS	PB
NB	(H,L)	(H,L)	(H,M)	(M,M)	(L,H)
NS	(H,L)	(H,M)	(M,M)	(L,M)	(L,H)
ZE	(H,M)	(M,M)	(L,M)	(M,M)	(H,M)
PS	(L,H)	(L,M)	(M,M)	(H,M)	(H,L)
PB	(L,H)	(M,M)	(H,M)	(H,L)	(H,L)

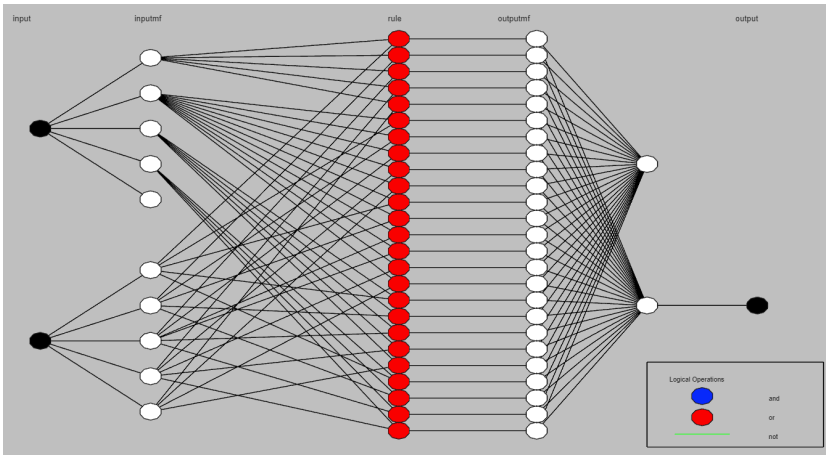


Figure 3. ANFIS structure implemented in MATLAB/ANFIS toolbox

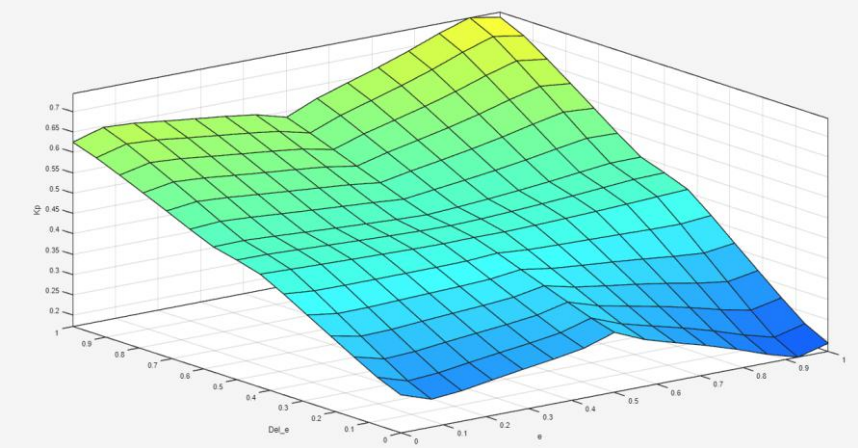


Figure 4. ANFIS rules 3D view

4. RESULTS AND DISCUSSION

The simulation was performed in MATLAB 2017b, and IEEE microgrid system 14 is considered for obtaining the desired results and compared results with and without implementing ANFIS-UPQC scheme. Figure 5 illustrates the simulation diagram of the microgrid test system integrated with the ANFIS-controlled UPQC (ANFIS-UPQC); i) case 1: base microgrid without UPQC (duration: 0–0.35 s); ii) case 2: voltage sag (applied at 0.05 s); iii) case 3: voltage swell (applied at 0.10 s); iv) case 4: variable load (load profile shown in Figure 6); and v) case 5: ANFIS-UPQC compensation (same disturbances applied, UPQC enabled).

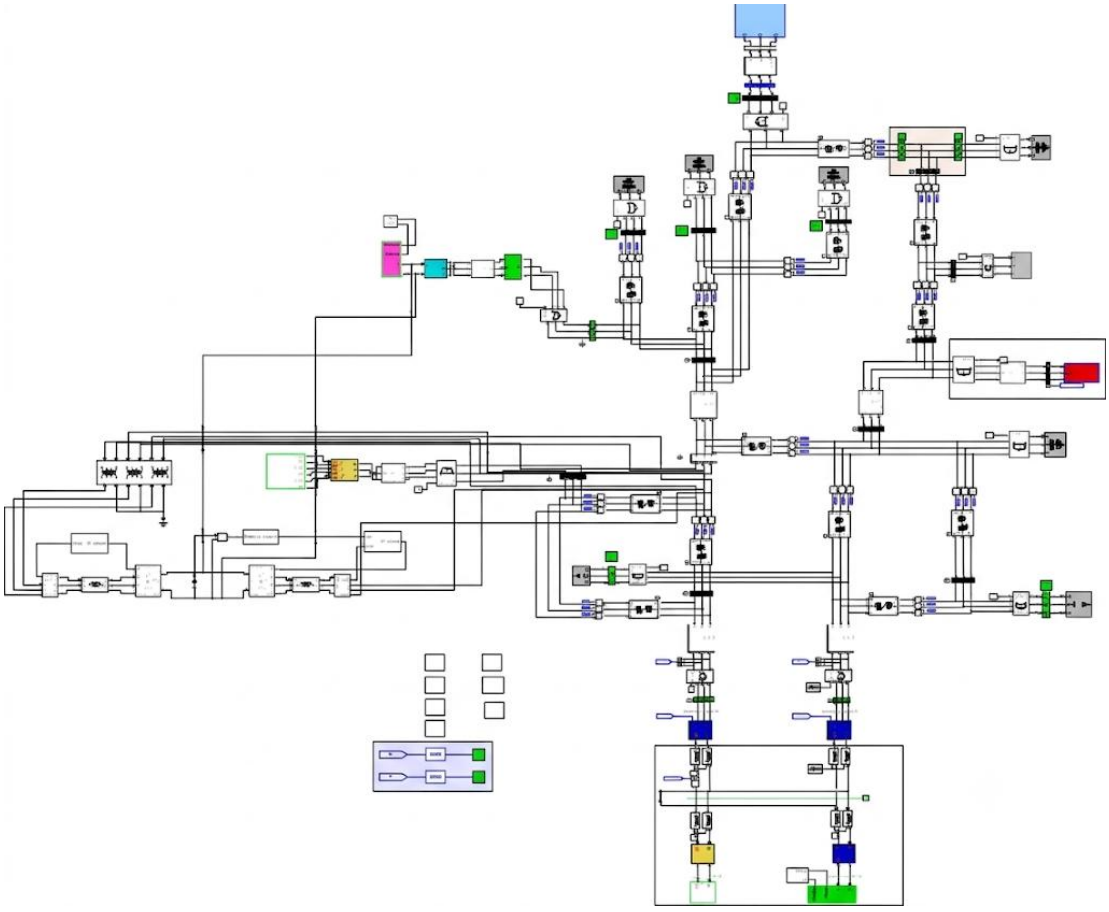


Figure 5. Modified IEEE 14-bus microgrid simulation model incorporating the ANFIS-controlled UPQC, adapted from [24]

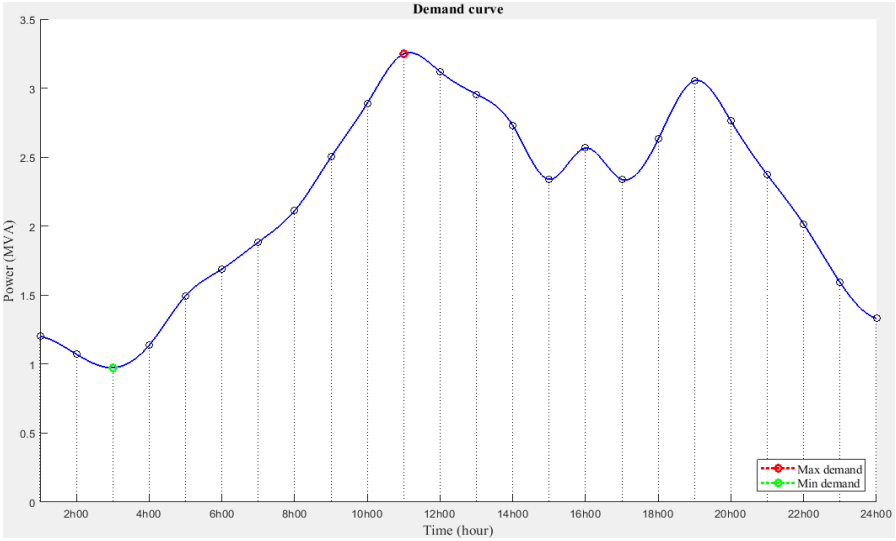


Figure 6. Hourly load in the microgrid

Bus 2 was selected as the UPQC installation point because it acts as a critical load bus located close to the point of common coupling and exhibits noticeable voltage fluctuations, reactive power demand, and current distortion under varying microgrid loading conditions. Installing UPQC at bus 2 enables simultaneous mitigation of upstream and downstream disturbances while maximizing compensation effectiveness throughout the network. The applied load pattern over a 0.35-second interval is depicted in Figure 6; it begins at a minimal value, reaches a peak, and subsequently drops back to a lower level.

Figure 7 presents the voltage amplitudes and unbalancing voltage deviation across all buses prior to compensation. Under these baseline conditions, the deviations are 0.046419 pu for Phase A, 0.032761 pu for Phase B, and 0.042813 pu for Phase C. Figure 8 highlights the corresponding power factors, showing that while buses 2 and 9 maintain a unity power factor, the remaining buses fall below 0.85. The impact of UPQC-ANFIS control is demonstrated in the subsequent results. Figure 9 shows the updated voltage amplitudes and voltage unbalance, where the unbalance deviations have successfully been reduced to 0.043969 pu (Phase A), 0.030103 pu (Phase B), and 0.040229 pu (Phase C). Furthermore, as seen in Figure 10, the power factor at buses 3 and 4 improves to above 0.86, with the other buses remaining unaffected by the UPQC intervention. Finally, Figure 11 confirms that the THD is maintained well within acceptable standard limits. Table 4 represent the comparison between the proposed and conventional technique.

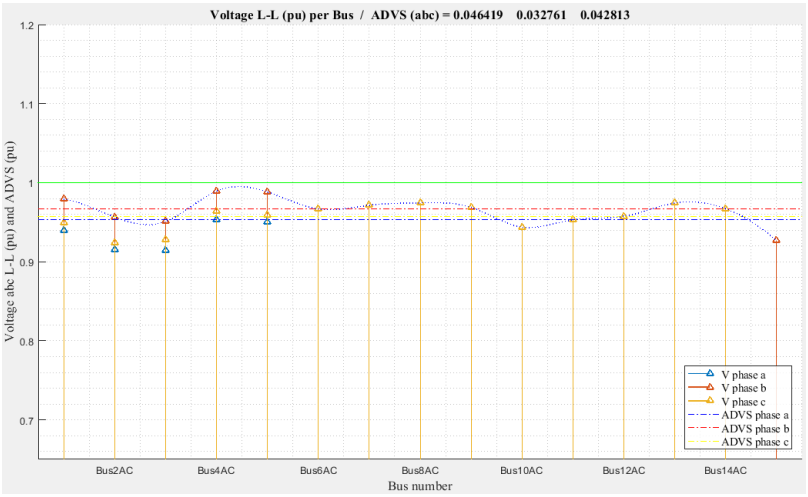


Figure 7. Unbalancing of voltage

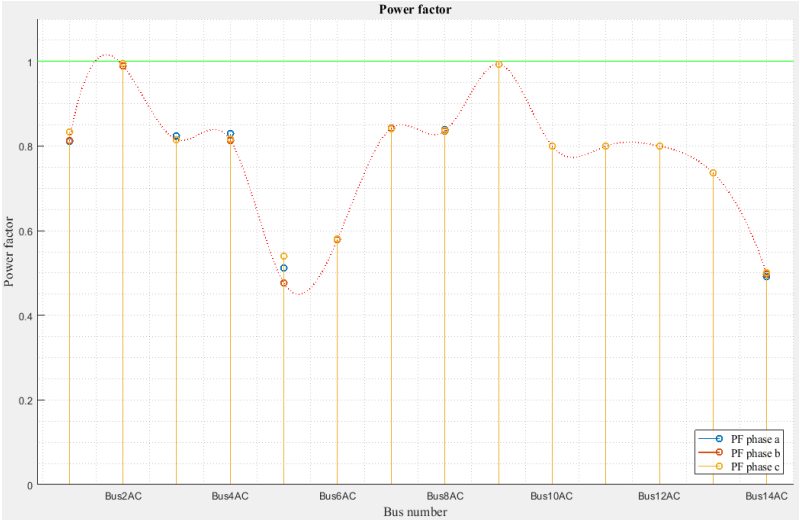


Figure 8. Power factor of the buses

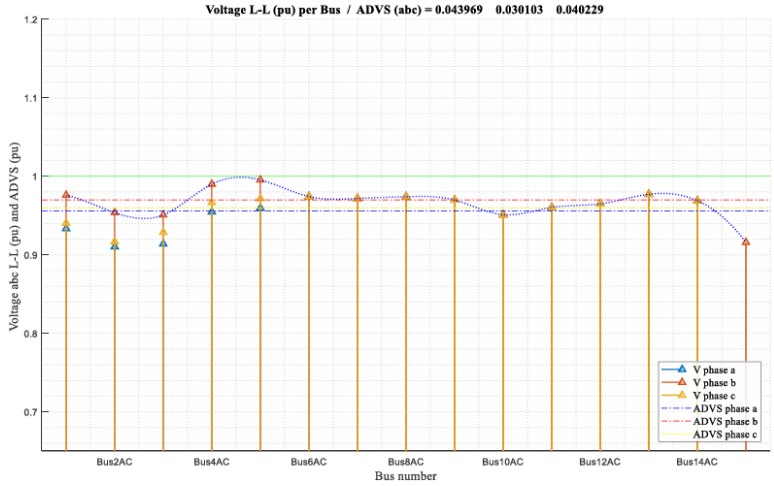


Figure 9. After applying ANFIS-UPQC control-voltage unbalancing

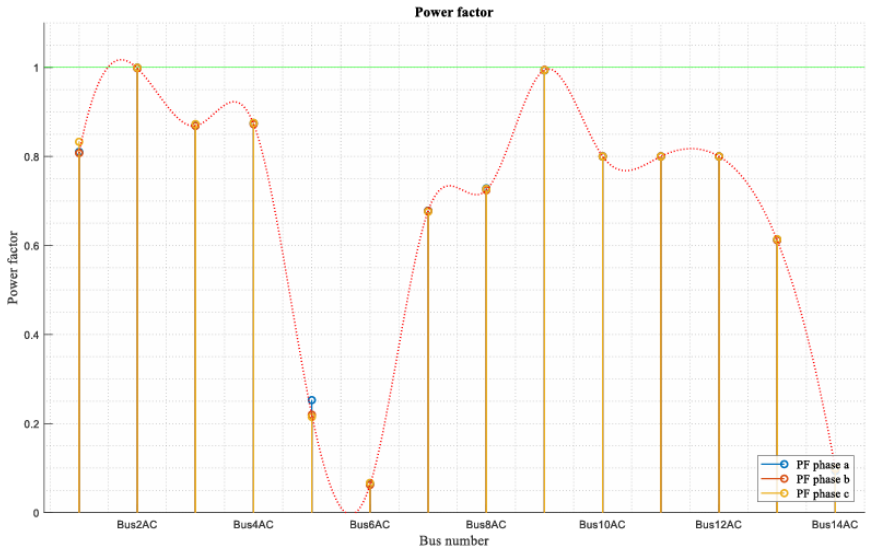


Figure 10. Power factor after ANFIS-UPQC

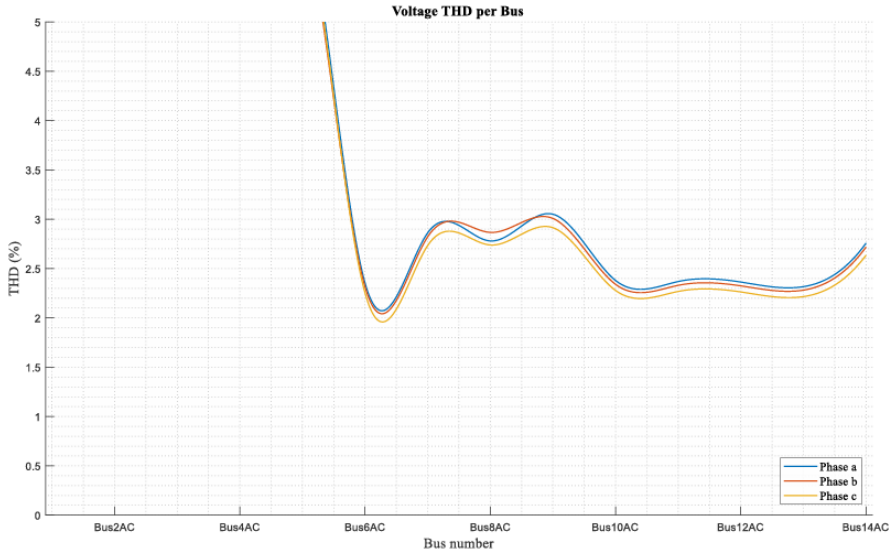


Figure 11. After connecting UPQC with ANFIS-THD values

Table 4. Power quality performance comparison

Parameter	Before compensation	After compensation	Improvement (%)
Voltage unbalance A	0.046419	0.043969	4.81
Voltage unbalance B	0.032761	0.030103	8.11
Voltage unbalance C	0.042813	0.040229	6.03
PF bus 3	<0.85	>0.86	1.18
PF bus 4	<0.85	>0.86	1.18
Reactive power	0.1	0	10

Figure 12 presents the real power, reactive power, voltage, and current profiles at bus 2 prior to the implementation of the UPQC-ANFIS controller. The data clearly shows disturbances in both real and reactive power, driven by voltage sag and swell events occurring at 0.05 s and 0.1 s, respectively.

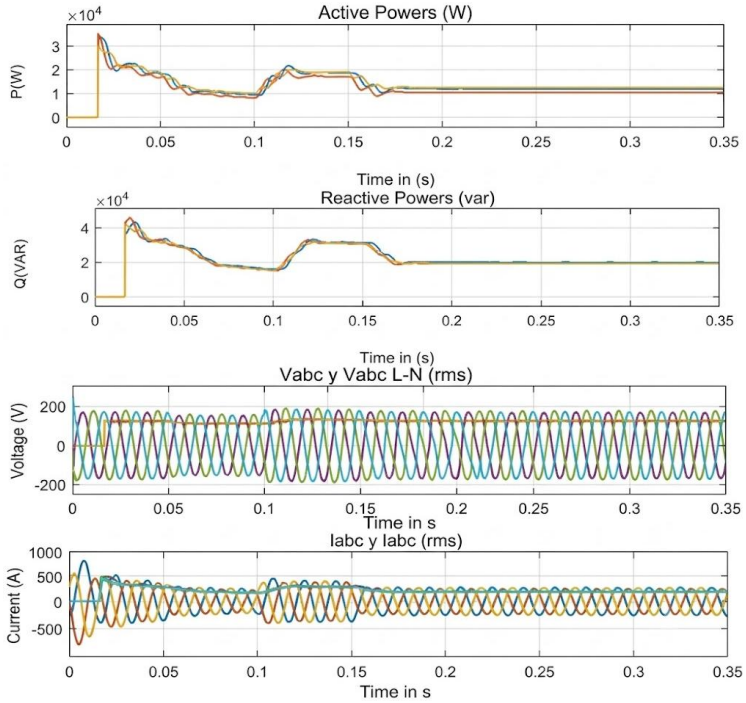


Figure 12. Before using UPQC and ANFIS

Figure 13 provides a magnified view of these uncompensated voltage fluctuations. Following the integration of the UPQC-ANFIS control, the system dynamics improved significantly, as illustrated in Figure 14. The reactive power is effectively neutralized, which subsequently leads to a drastic reduction in current amplitude. Moreover, the voltage waveform demonstrates successful compensation of the initial sag and swell conditions, a correction that is clearly visible in the zoomed-in view provided in Figure 15. Overall, these results successfully validate the performance of the PV-powered, ANFIS-controlled UPQC in stabilizing the testbed.

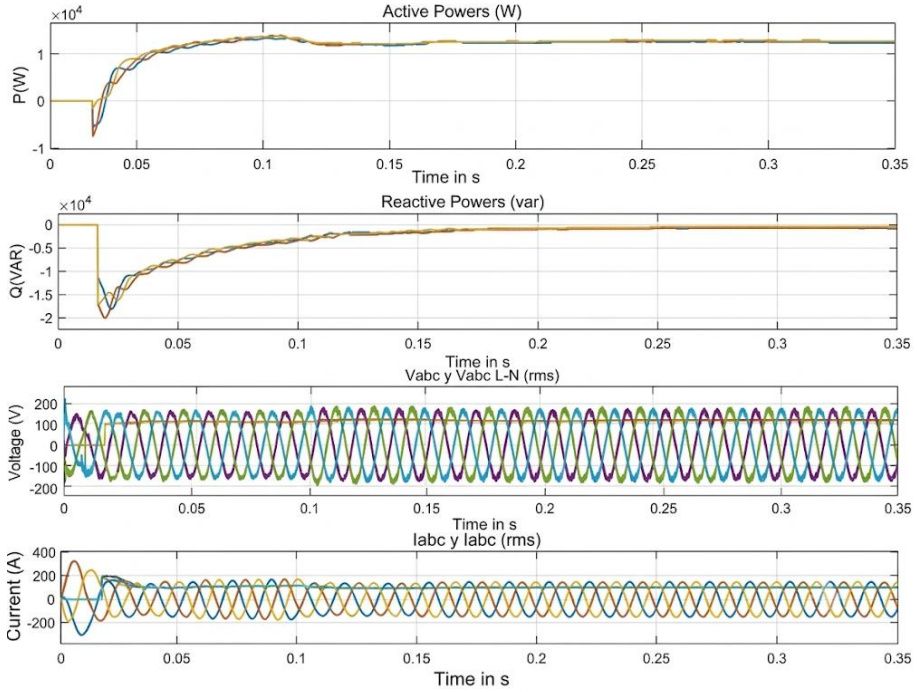


Figure 13. After using UPQC and ANFIS

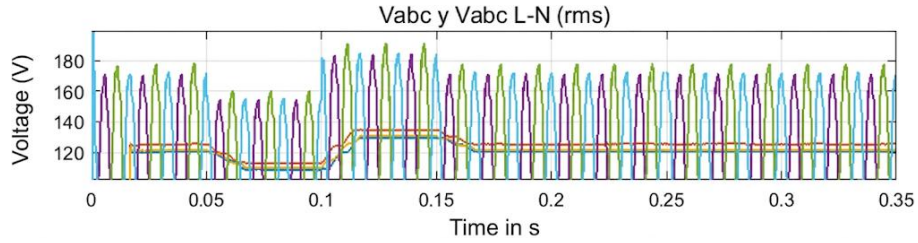


Figure 14. Zoomed view of bus no. 2 without UPQC and ANFIS

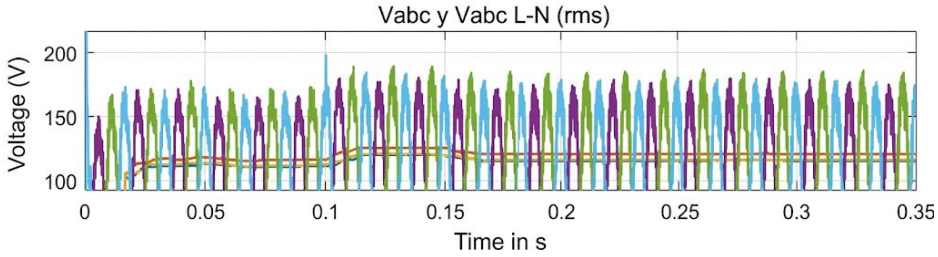


Figure 15. After connecting UPQC and ANFIS

The proposed controller reduced voltage imbalance by 4.81%, 8.11%, and 6.03% in phases R, Y, and B, respectively. Additionally, power factor values improved from less than 0.85 to greater than 0.86 at buses 3 and 4, demonstrating enhanced reactive power compensation capability. Table 5 represents the comparison of the proposed method with previous methods. The present study is limited to MATLAB/Simulink-based

verification using a standard IEEE microgrid model. Practical implementation challenges such as converter nonidealities, sensor noise, communication delays, synchronization errors, and real-time computational constraints have not been considered. The parameters used in the simulation is depicted in Table 6.

Table 5. Comparison with existing control strategies

Feature	PI-UPQC	Fuzzy-UPQC	ANN-UPQC	Proposed ANFIS-UPQC
Adaptability	Low	Medium	High	Very high
Nonlinear handling	Low	High	High	Very high
Learning capability	No	No	Yes	Yes
Rule interpretability	No	Yes	No	Yes
PQ improvement	Moderate	High	High	Higher
Computational burden	Low	Medium	High	Medium

Table 6. Parameter for simulation

Equipment	Parameters	Values
PV rating	Voc	37.2 V
	Vmp	30.2 V
	Isc	8.62 A
	Imp	8.1 A
	Number of series connections	20
	Number of parallel connections	2
Boost converter	Inductor	12 µH
	Frequency	5 kHz
EV charger	Inductor	0.03 mH
	Capacitor	2200 µF
	Frequency	20 kHz
EV battery	Type	li-io
	Nominal voltage	48 V
	Rated capacity	500 Ah

5. CONCLUSION

To validate the performance of the PV-powered, ANFIS-controlled UPQC, we utilized the standard microgrid model. Bus 2 was specifically selected for the UPQC placement because it operates at 220 V, representing a typical distribution point where power quality issues most frequently occur. The simulation results demonstrate that the UPQC performs exceptionally well at this node, effectively compensating for voltage sags and swells while simultaneously improving the power factor and reducing THD. Furthermore, by actively neutralizing reactive power, the system substantially reduces the peak current drawn by the microgrid. Ultimately, the implementation of this ANFIS-controlled framework yields a significant positive impact on the overall stability and efficiency of the microgrid network.

The implementation of the ANFIS-UPQC resulted in a noticeable reduction in voltage unbalance across all phases. The voltage unbalance deviation decreased from 0.046419 pu to 0.043969 pu in Phase A, from 0.032761 pu to 0.030103 pu in Phase B, and from 0.042813 pu to 0.040229 pu in Phase C, corresponding to improvements of 4.81%, 8.11%, and 6.03%, respectively. Moreover, the power factors at buses 3 and 4 increased from values below 0.85 to above 0.86, indicating a minimum improvement of approximately 1.18%. These results demonstrate the effectiveness of the proposed ANFIS-UPQC controller in enhancing voltage balance and power quality within the microgrid system.

The proposed ANFIS-UPQC controller demonstrates considerable potential for improving power quality and operational reliability in microgrid systems. By effectively mitigating voltage unbalance and enhancing power factor levels, the controller contributes to a more stable and efficient power distribution environment. These improvements can support the integration of renewable energy sources and sensitive loads by reducing power quality disturbances and ensuring better utilization of electrical infrastructure. Furthermore, the adaptive learning capability of the ANFIS-based control strategy enables UPQC to respond effectively to varying operating conditions, making it a suitable solution for modern smart grid and microgrid applications. Overall, the proposed approach offers a practical and robust framework for enhancing system performance, reliability, and power quality in distributed energy networks.

However, the investigation is limited to simulation studies; therefore, the practical performance under measurement uncertainties and hardware constraints remain unverified. Future work will focus on hardware-in-the-loop validation, experimental implementation, evaluation under fluctuating renewable generation and dynamic load conditions, and comparison with advanced intelligent controllers such as deep learning, reinforcement learning, and model predictive control approaches.

ACKNOWLEDGMENTS

We acknowledge our supervisor and family members for their support.

FUNDING INFORMATION

This is self-funded research.

AUTHOR CONTRIBUTIONS STATEMENT

This journal uses Contributor Roles Taxonomy (CRediT) to recognize individual author contributions, reduce authorship disputes, and facilitate collaboration.

Name of Author	C	M	So	Va	Fo	I	R	D	O	E	Vi	Su	P	Fu
Jabinbanu Mahaboobsab Nadaf	✓	✓	✓	✓	✓	✓	✓	✓	✓	✓			✓	✓
Sudarshana Reddy Handihal Rukmangada		✓				✓		✓	✓	✓	✓	✓		
Suresh Haleyur Lakshmegowda		✓				✓		✓	✓	✓	✓			

C : **C**onceptualization
M : **M**ethodology
So : **So**ftware
Va : **Va**lidation
Fo : **Fo**rmal analysis
I : **I**nvestigation
R : **R**esources
D : **D**ata Curation
O : Writing - **O**riginal Draft
E : Writing - Review & **E**diting
Vi : **Vi**sualization
Su : **Su**pervision
P : **P**roject administration
Fu : **Fu**nding acquisition

CONFLICT OF INTEREST STATEMENT

Authors state no conflict of interest.

DATA AVAILABILITY

Data can be sent through email to the readers if they ask through email.

REFERENCES

[1] B. Chaudhari, "A Review on Development in Unified Power Quality Conditioner," *J. Electr. Syst.*, vol. 20, no. 3, pp. 4655–4673, Apr. 2024, doi: 10.52783/jes.5833.
[2] Y. Mei, J. Xu, C. Peng, W. Kong, G. Peng, and G. Song, "Voltage quality enhancement of distribution network based on unified power quality conditioner with BESS," *Front. Energy Res.*, vol. 12, Sep. 2024, doi: 10.3389/fenrg.2024.1472503.
[3] T. Wu, S. Huang, and P. Chen, "Application of a three-phase unified power quality conditioner in a microgrid," *IET Smart Grid*, vol. 7, no. 6, pp. 872–890, Dec. 2024, doi: 10.1049/stg2.12184.
[4] L. G, R. D. D, V. K, N. V. Gour, M. R, and S. D. S, "Hybrid Optimization of Unified Power Quality Conditioner Placement for Enhanced Grid Performance," *Int. J. Electr. Electron. Eng.*, vol. 12, no. 3, pp. 74–83, Mar. 2025, doi: 10.14445/23488379/IJEEE-V12I3P108.
[5] K. Sarker, J. Sarker, K. Sarkar, D. Chatterjee, and P. Bhowmik, "Power Quality Enhancement in Smart Grids Using DFIG-PV-IG Integrated UPQC with Unequal Step Multilevel Inverter for Sensitive Electric Vehicle and Medical Loads," *Arab. J. Sci. Eng.*, vol. 51, no. 8, pp. 10747–10778, Apr. 2026, doi: 10.1007/s13369-025-10817-3.
[6] A. J. Patel and A. V. Sant, "Moving Window Min-Max Algorithm-Based Control of UPQC at EV Charging Station," in *Proc. IEEE 3rd Int. Conf. Smart Technol. Power Energy Control (STPEC)*, 2023, pp. 1-6, doi: 10.1109/STPEC59253.2023.10430760.
[7] C. S. V. P. Rao, A. Pandian, C. R. Reddy, M. Bajaj, J. Massoud, and M. Shouran, "Unified power quality conditioner-based solar EV charging station using the GBDT–JS technique," *Front. Energy Res.*, vol. 12, Apr. 2024, doi: 10.3389/fenrg.2024.1343635.
[8] K. Srilakshmi *et al.*, "Optimal design of solar/wind/battery and EV fed UPQC for power quality and power flow management using enhanced most valuable player algorithm," *Front. Energy Res.*, vol. 11, Jan. 2024, doi: 10.3389/fenrg.2023.1342085.
[9] K. M. S. Kumar, S. Das, R. K. Lenka, and R. Patel, "Robust Control Strategy for PV-Battery Integrated UPQC in Electric Vehicle Charging Stations for Power Quality Enhancement," in *Proc. Int. Conf. Power Electron. Energy (ICPEE)*, 2025, pp. 1–6, doi: 10.1109/ICPEE65973.2025.11411125.
[10] S. S, T. H, S. J, and S. R. Gunaga, "Fuzzy proportional-integral controlled unified power quality conditioner for electric vehicle charging grids," *Int. J. Electr. Comput. Eng.*, vol. 15, no. 4, p. 3527, Aug. 2025, doi: 10.11591/ijece.v15i4.pp3527-3535.
[11] Y. V. P. Kumar *et al.*, "Fuzzy Hysteresis Current Controller for Power Quality Enhancement in Renewable Energy Integrated Clusters," *Sustain.*, vol. 14, no. 8, p. 4851, 2022, doi: 10.3390/su14084851.
[12] R. Senapati, R. N. Senapati, and M. K. Moharana, "Sinusoidal Current Control Strategy for UPQC in Grid Connected PV-Fuel Cell Microgrid," *Int. J. Eng. Technol.*, vol. 9, pp. 2800–2813, 2017.
[13] H. Li, Y. Zhang, S. Yang, and X. Liu, "High-resolution Dataset of Electric Vehicle Charging Responses Under Varied Power Quality Disturbances," *Sci. Data*, vol. 13, no. 403, Feb. 2026, doi: 10.1038/s41597-026-06768-5.

[14] A. F. M. Correia *et al*., "Architecture and Operational Control for Resilient Microgrids—A University Case Study," *IEEE Access*, vol. 13, pp. 51373-51387, 2025, doi: 10.1109/ACCESS.2025.3553350
[15] J. M. Guerrero, M. Chandorkar, T.-L. Lee, and P. C. Loh, "Advanced Control Architectures for Intelligent Microgrids—Part I: Decentralized and Hierarchical Control," *IEEE Trans. Ind. Electron.*, vol. 60, no. 4, pp. 1254–1262, Apr. 2013, doi: 10.1109/TIE.2012.2194969.
[16] M. Uddin, H. Mo, D. Dong, S. Elsawah, J. Zhu, and J. M. Guerrero, "Microgrids: A review, outstanding issues and future trends," *Energy Strategy Rev*, vol. 49, 2023, doi: 10.1016/j.esr.2023.101127.
[17] T. Adefarati and R. C. Bansal, "Integration of renewable distributed generators into the distribution system: a review," *IET Renew. Power Gener.*, vol. 10, no. 7, pp. 873–884, Aug. 2016, doi: 10.1049/iet-rpg.2015.0378.
[18] M. Panda, M. Chankaya, S. Mohanty and S. D. Sandeep, "State-of-Charge-Based Energy Management Strategy for Hybrid Energy Storage System in DC Microgrid," *IEEE Access*, vol. 13, pp. 77353-77364, 2025, doi: 10.1109/ACCESS.2025.3564786.
[19] M. Shahidehpour, Z. Li, and M. Ganji, "Smart cities for a sustainable urbanization: Illuminating the need for establishing smart urban infrastructures," *IEEE Electrif. Mag.*, vol. 6, no. 2, pp. 16–33, Jun. 2018, doi: 10.1109/MELE.2018.2816840.
[20] A. Bidram, F. L. Lewis, and A. Davoudi, "Distributed control systems for small-scale power networks: Using multiagent cooperative control theory," *IEEE Control Syst.*, vol. 34, no. 6, pp. 56–77, Dec. 2014, doi: 10.1109/MCS.2014.2350571.
[21] Y. Han, H. Li, P. Shen, E. A. A. Coelho, and J. M. Guerrero, "Review of Active and Reactive Power Sharing Strategies in Hierarchical Controlled Microgrids," *IEEE Trans. Power Electron.*, vol. 32, no. 3, pp. 2427–2451, Mar. 2017, doi: 10.1109/TPEL.2016.2569597.
[22] A. G. Tsikalakis and N. D. Hatziargyriou, "Centralized control for optimizing microgrids operation," in *2011 IEEE Power and Energy Society General Meeting*, IEEE, Jul. 2011, pp. 1–8, doi: 10.1109/PES.2011.6039737.
[23] E. Hossain, E. Kabalci, R. Bayindir, and R. Perez, "Microgrid testbeds around the world: State of art," *Energy Convers. Manage.*, vol. 86, pp. 132–153, 2014, doi: 10.1016/j.enconman.2014.05.012.
[24] L. Ortiz, R. Orizondo, A. Águila, J. W. González, G. J. López, and I. Isaac, "Hybrid AC/DC microgrid test system simulation: grid-connected mode," *Heliyon*, vol. 5, no. 12, p. e02862, Dec. 2019, doi: 10.1016/j.heliyon.2019.e02862.
[25] A. Jabbar, A. Y. Elrayyah, M. Z. C. Wanik, A. Sanfilippo, and N. Singh, "Development of Hybrid AC/DC Laboratory-scale Smart Microgrid Testbed with Control & Monitoring System Implementation in LabVIEW," *Int. J. Hydrol. Environ. Sustain.*, 2019, pp. 889–894, doi: 10.1109/GTDAsia.2019.8715942.

BIOGRAPHIES OF AUTHORS



Jabinbanu Mahaboobsab Nadaf obtained a Master of Technology degree from Visvesvaraya Technological University, Belgaum. She served as lecturer senior grade and selection grade levels in the Department of Technical Education, Government of Karnataka, India. Presently she is working as head of the Department of Electrical and Electronics Engineering at Sri Channakeshava Government Polytechnic, Guddadachannapur, Bankapur, Karnataka, India. She is a research scholar at University BDT College of Engineering, a constituent college of Visvesvaraya Technological University, Belgaum, Karnataka, India. Her research interests include optimal power flow management in smart-grid-connected renewable energy resources, smart grid integration, and renewable energy. She can be contacted at email: jabinbanu.nadaf5976@gmail.com.



Dr. Sudarshana Reddy Handihal Rukmangada is a professor in the Department of Electrical and Electronics Engineering, UBDT College of Engineering, Davangere, a constituent College of Visvesvaraya Technological University, Belgaum, Karnataka, India. Presently he is working as regional director Visvesvaraya Technological University Regional Office, Bengaluru, Karnataka, India. His research interests include advances of smart grid connected renewable energy in power system engineering, distributed generation, and power system stability analysis. He can be contacted at email: hrsreddy@gmail.com.



Dr. Suresh Haleyur Lakshmegowda a professor and head of the Department of Electrical and Electronics Engineering, Sir M Visvesvaraya Institute of Technology, Bangalore, Karnataka, India. His research interests include reactive power compensation, renewable energy and smart grid integration, and EV technology. He can be contacted at email: dr.hlsuresh_eee@sirmvit.edu.